13th International Conference on
Structural Health Monitoring of Intelligent Infrastructure
DOI: 10.3217/978-3-99161-057-1-013

Finite element mesh construction for seismic analysis using drone imagery

Evan T. Delaney[1], Patrick Marty[1], Lars Gebraad[2], Andrea Zunino[1], Andreas Fichtner[1]
[1]Institute of Geophysics, Department of Earth and Planetary Sciences, ETH Zurich, Sonneggstrasse 5, 8092 Zurich, Switzerland
[2]Mondaic AG, c/o Impact Hub Zurich, Sihlquai 131, 8005 Zurich, Switzerland
email: delaneye@student.ethz.ch, patrick.marty@eaps.ethz.ch, lars.gebraad@mondaic.com, andrea.zunino@eaps.ethz.ch, andreas.fichtner@eaps.ethz.ch

ABSTRACT: Computational meshes serving as input to wave simulations are often crafted manually and bear a significant cost to construct. The aim of this work is to minimize that overhead and apply it to structures lacking models and meshes, particularly in earthquake-prone regions, to image and monitor their structural health in response to ground movement. To address this challenge, we have developed a workflow to facilitate the creation of 3D finite element meshes, starting with 2D photos acquired by an inexpensive consumer-level unmanned aerial system (i.e., a drone). After photo acquisition, the process proceeds by utilizing computer graphics and vision software to transform these photos into a 3D surface composed of triangles. Surface meshes are generally sufficient products for other workflows that likewise create 3D assets via reconstruction methods (e.g., for topographic mapping, archiving, and entertainment). However, to simulate waves through complex structures with high fidelity, we employ a spectral element wave solver, which requires a 3D volume composed of hexahedra. The steps from a 3D triangular surface to a 3D hexahedral volume include enclosing the surface, conditioning, and remeshing it with appropriate element geometry. We apply a first version of this workflow to the Contra (Verzasca) dam in Switzerland, from which we discuss key stages, challenges, and learnings in developing the pipeline – showcasing elastic wave simulation through the constructed mesh.

KEY WORDS: Photogrammetry; UAS; UAV; Gridding; Meshing; Numerical modelling; Geophysics; Seismology.

1 INTRODUCTION

Seismological research focused on understanding the behavior of complex media and structures to ground motion requires the use of computational meshes, which permit the physical world to be discretized in order to numerically solve the wave equation. These meshes must be constructed in a way that not only honors structural topography and field parameters, but also maintains efficiency, preserves the physics, and upholds numerical stability requirements dictated by grid size, frequency, and velocity parameters [1,2]. When no compatible computational mesh or model exists for the object or area of interest, a mesh must then be constructed from scratch. This is an arduous task for geoscientists, being a bottleneck for those wishing to focus their attention on imaging the Earth and likewise on deriving insights from the non-destructive testing of engineering structures and their responses to earthquakes.

A proposed solution to this challenge is a workflow that incorporates the use of unmanned aerial vehicles (i.e., UAVs, unmanned aerial systems (UASs), or drones) along with computer vision and graphics software to process the imagery and generate meshes for wave propagation and seismic research problems. Significant advances in hardware (e.g., digital cameras, GPS, drone portability, etc.) have opened the door to more flexibly capture thousands of images without resorting to expensive equipment, non-trivial calibration methods, and the use of priors (e.g., camera settings, motion, etc.) [3-6]. This lower barrier to entry has furthermore been complemented by improvements in key computer vision algorithms (namely, Structure-from-Motion and Multi-View Stereo) which now make it practical to reconstruct 3D surface models from these thousands of images using a high-end laptop or modest workstation [7].

We develop a first iteration of this workflow and apply it to the Contra dam located in the Verzasca valley in southern Switzerland, whose results we present. This structure and its surroundings have no known mesh, making it an ideal candidate to qualify whether it is possible to generate a useable mesh with minimal effort via these off-the-shelf and improved technologies.

2 WORKFLOW AND RESULTS

2.1 Methodology

The workflow to generate a computational-ready mesh for input into a spectral element wave solver, as applied to the Contra dam, is as follows:

1) identifying the object or area of interest
2) survey design
3) photo acquisition
4) color calibration
5) surface model generation
6) surface model enclosing
7) conditioning and layer additions
8) hexahedral remeshing
9) populating field parameters

We now proceed in the following paragraphs to describe these steps in further detail.

2.1.1.a Identifying the object or area of interest

The Contra dam is selected as a test candidate, given the fact that it lies within a seismically active region and lacks a mesh for itself and its surrounding environment. Located near the city of Locarno, it is embedded in somewhat steep mountain flanks with outcropping metamorphic synfolds [8,9]. At the time of acquisition, the dam was undergoing maintenance with the

DOI: 10.3217/978-3-99161-057-1-013

reservoir (Lago di Vogorno) drained to allow for an acquisition of not only the dam, but also the lakebed topography leading into the dam. The field site is presented in Figure 1.

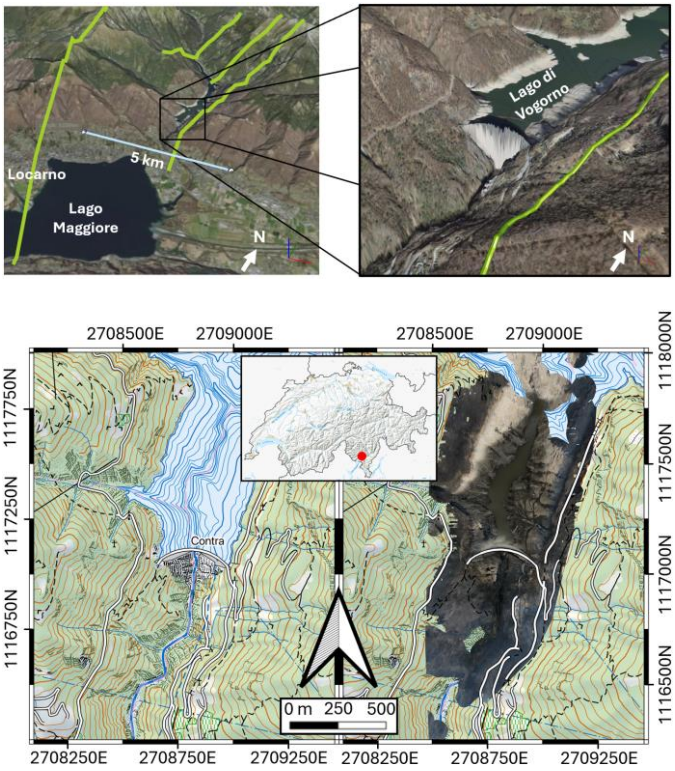

Figure 1. (top left) Location of the Contra dam zoomed out and in respect to the city of Locarno to its southwest. The light teal line represents 5 km. Lime lines are mapped faults. (top right) A zoomed view of the area, as taken from swisstopo, with the dam near the center and the reservoir Lago di Vogorno behind. The lime polyline to the right of the dam is the edge of a mapped fault. (bottom left) A terrain map of the field site. (bottom right) A reconstructed orthophoto overlain revealing the drained lakebed.

2.1.1.b Survey design

Data are collected with significant overlap among the photos such that common features could be identified. We achieve this by flying at different heights and by also adjusting the camera's angle. For the drone, we choose the DJI Mavic Air 2, retailing for under 1000 USD. With a field-of-view of 84° and given a fixed f//2.8 aperture with equivalent focal length of 24mm, this brand of drone gives us the flexibility to acquire photos from seven meters or greater to achieve a reasonable depth of field, which is vital in the later step of identifying common features among the fore-, mid-, and backgrounds. In terms of acquisition paths, we opt for circular and linear hyperlapse defaults as found within the drone's support software. We do not use ground control points or calibration tables.

We additionally plan and coordinate with the dam operators and Locarno air traffic control prior to and during acquisition.

2.1.1.c Photo acquisition

During a period of three hours, we pilot a Mavic Air 2 drone and use its camera to acquire 1143 images at 12 MP (4000 x 3000 MP). We select a shutter speed of 1/640 s and a 100 ISO setting due to sunny conditions. A subset of the acquired photos is given in Figure 2.

Figure 2. Various photos of the dam and lakebed as taken from a drone.

2.1.1.d Color calibration

Having acquired the photos on a sunny day over a few hours, we observe inconsistent lighting (Figure 2). As this may hinder mesh reconstruction [10], we apply basic post-photo processing to correct for various degrees of whiteness, brightness, and moving shadows.

2.1.1.e Surface model generation

Multiple photogrammetry software options (WebODM, Meshroom, RealityCapture, and Metashape) are evaluated in terms of their speed, accuracy, ease-of-use, functionality, and of particular concern, ability to reconstruct 3D surface meshes with minimal topological issues (e.g., holes). RealityCapture (RC) and Metashape perform the best, with RC having the added benefit of being free. However, RC only runs on Windows and requires an Nvidia CUDA GPU. But due to clever memory management, RC does not require significant amounts of RAM. Metashape can run on Linux, Mac, and Windows, with RAM demands scaling with number of 2D photos. We move forward with a 3D surface mesh created in Metashape on a 16-core CPU/40-core GPU M3 Max MacBook Pro laptop with 64 GB of unified memory shared between the CPU and GPU. The photogrammetry process of importing photos, to feature matching, to image alignment, to the eventual mesh generation, decimation, and smoothing requires less than thirty minutes to complete.

2.1.1.f Surface model enclosing

To perform 3D wave simulations using the spectral element method, we require a volumetric mesh and not a surface mesh. Our workflow uses a specific implementation of the spectral element method called Salvus [11], which requires a mesh either composed of hexahedra if solving 3D wave solutions or quadrilaterals for 2D problems. The reason for this is to exploit a fundamental benefit of using spectral element methods for wave propagation modelling: 2D quads or 3D hexes result in a diagonal mass matrix and thus trivialize inverting the mass matrix [11-13]. Given the 3D nature of our dam, we take the 3D triangular surface mesh from 2.1.1.e and extrude the mesh outwards and downward before sealing the base, thus creating

DOI: 10.3217/978-3-99161-057-1-013

a watertight 3D surface mesh. This is accomplished using Blender, a free and open-source 3D computer graphics software package [14].

2.1.1.g Conditioning and layer additions

Before converting the 3D enclosed surface mesh of triangles into a 3D volumetric mesh of hexes, we further correct for any additional topology issues using Blender's 3D sculpting tools and then remesh the surface into quads. Any unhandled spikes or non-physical geometries may result in bad elements (with small or negative Jacobians – i.e., squished elements) which would render subsequent wave simulations infeasible. And the reason for converting from triangles to quads is that the next step more robustly remeshes when given a quad surface. Once satisfied with the mesh, we add a water layer on top.

2.1.1.h Hexahedral remeshing

The surface mesh is then transformed into a volumetric hexahedral mesh using Cubit, a meshing software tool developed to create tetrahedral and hexahedral meshes for finite element analysis and fluid dynamics [15]. To preserve the topography of the dam and the surface, we choose an element size of approximately 2.5 m x 2.5 m x 2.5 m. Based on results at this stage, an iterative process takes place by returning to 2.1.1.d to further improve the quality of this mesh. We accomplish this by conditioning the surface mesh in a manner that prevents Cubit from outputting volumetric meshes containing elements with a small Jacobian, as these elements are unphysical or dimensioned smaller than desired. A smaller element size dictates a decrease in timestep, which adversely increases simulation time and memory requirements. Results from steps 2.1.1e to 2.1.1h are presented in Figure 3.

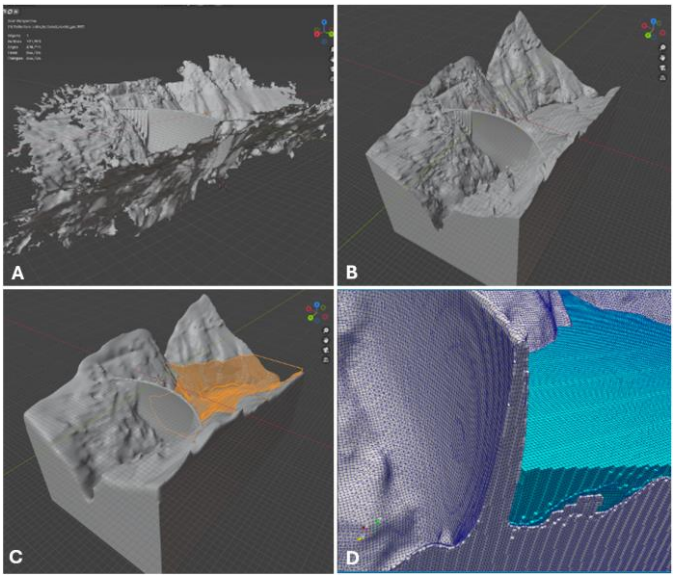

Figure 3. (A) displays the 3D surface mesh output as described in section 2.1.1e; (B) is the result of enclosing that surface mesh as detailed in section 2.1.1f; (C) shows a despiked and smoother version of (B) with the inclusion of a water layer in orange as noted in section 2.1.1.g; and (D) is an arbitrary slice through the hexahedral mesh, with bedrock and dam in gray and the water layer in blue as discussed in section 2.1.1h.

2.1.1.i Population field and simulation parameters

To qualify the mesh, we must populate it with elastic field parameters. We use a homogeneous compressional velocity of 4800 m/s, shear velocity of 2800 m/s, and density of 2710 kg/m^3 for the basement bedrock and dam. The water layer is given a sonic velocity of 1500 m/s and density of 1000 kg/m^3.

2.2 Simulation

The prepared mesh can now be used as input to the wave solver. For illustrative purposes, we initiate a 130 Hz Ricker spherical explosive point source (i.e., the curl of displacement is zero in an elastic homogeneous model). Dirichlet boundary conditions are assigned to the water-air, dam-air, and basement-air interfaces, and absorbing boundaries are placed on the other outer faces. Snapshots in both 2D and 3D are showcased in Figure 4. The mesh thus succeeds in allowing a solution to the wave equation, thus validating the workflow for this use case.

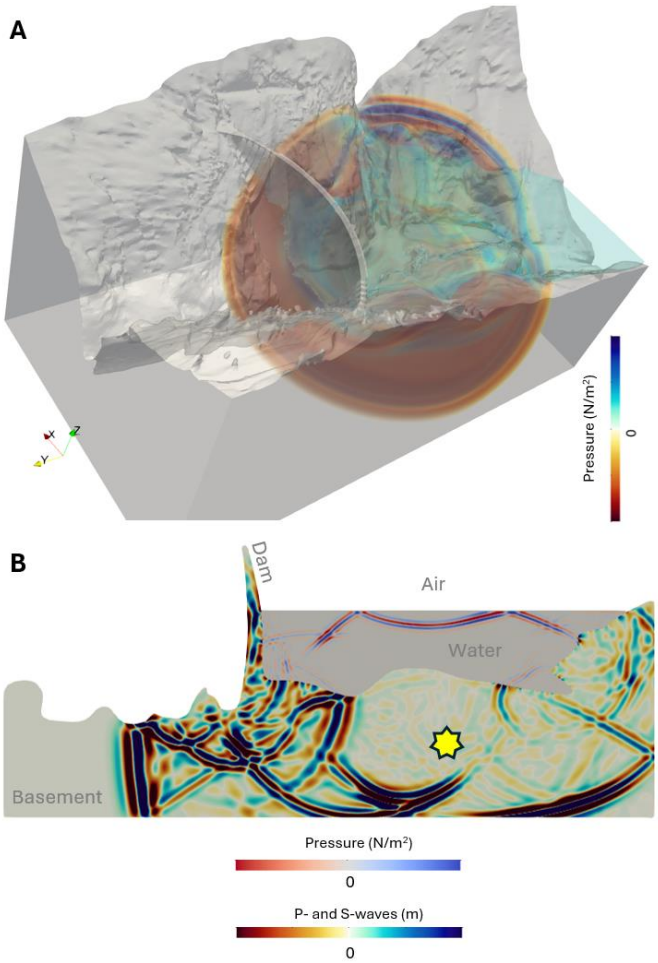

Figure 4. (A) shows a snapshot of an acoustic wavefield successfully propagating through the 3D mesh created from a drone photo acquisition. (B) is a slice through that 3D model at a later timestep to showcase various wave modes propagating through different media and structures in the model due to a point source activated at an earlier time at the location given by the yellow star. Waves within the water column are measured in pressure, whereas within the basement and dam they are given in terms of compressional and shear wave particle displacement.

DOI: 10.3217/978-3-99161-057-1-013

3 DISCUSSION

3.1 Alternative acquisition methods and inputs

Though the workflow emphasizes the use of drones to acquire photos as input, this is not a requirement. In fact, a LiDAR system, a phone camera, and other capture methods and tools could be employed – each with its own trade-offs [7]. We also consider the use of satellite imagery to construct a usable mesh. Unfortunately, it does not yield the necessary 3D detail or resolution to faithfully recover the dam and surrounding topography – which are paramount in ground motion studies [11,16,17]. Furthermore, satellite imagery is unable to capture complex 3D surface structures such as the dam's overhang. Figure 5 compares surface meshes created from various satellite sources to that generated from drone imagery.

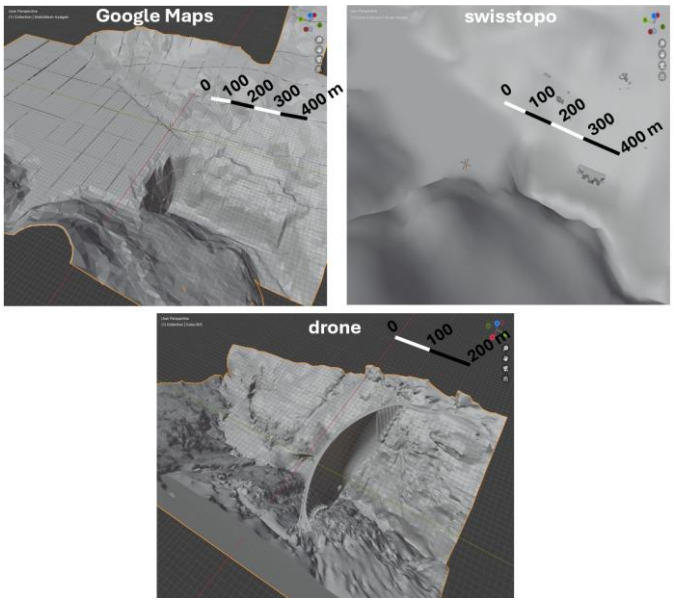

Figure 5. A comparison of different surface meshes created using satellite imagery input from Google Maps and swisstopo to that generated from drone imagery. There is added serendipity in having acquired the drone footage during dam maintenance. Meshes are displayed in perspective view.

3.2 Seismic hazard and risk analysis

We now have a beneficial workflow that substantially reduces the burden of constructing meshes. This leaves us with ample time to prioritize our focus on other problems within seismology. One of these problems includes quantifying ground shaking and its impacts on the environment.

As an example, we may now compute ground acceleration in our model and hypothetically venture to assess the risk of structural failure. For this demonstration, we simulate two different rupture sites at the dam and note the acceleration values that the dam and the bedrock (basement) may experience, as given in Figure 6. Analyzing the wavefields further would allow one to compute peak ground acceleration (PGA) values as input to probabilistic hazard and risk calculations [18]. As can be observed, ground motion values are amplified and dampened by many factors, including the topography, orientation of the rupture mechanism, and the presence of air or water at an interface.

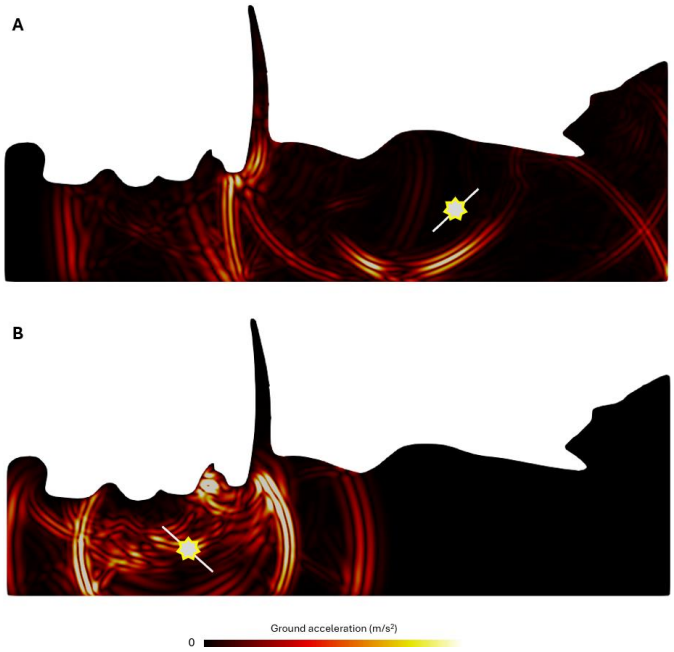

Figure 6. Magnitude of ground acceleration from two different sources, with snapshots taken near peak acceleration within the dam region for each scenario. Earthquake rupture location is indicated with a star, along with its orientation. The source at (A) is located farther from the dam and is underneath a water layer with smoother topography. (B)'s source lies closer to the dam below an air interface with rougher topography.

4 CONCLUSION

We provide a workflow outlining how images acquired from drones can be leveraged to create hexahedral meshes that may serve as input to wave simulations, successfully applying it to the Contra dam in Switzerland. The workflow has many steps, all of which may be readily accomplished by performing minor tweaks to off-the-shelf technologies. For situations where no computational mesh exists, acquiring the photos may take no more than a day or two – and in our case three hours. Given proficiency with the tools in the workflow, the simulation-ready mesh may be created in under a week, which marks a substantial improvement to the process of manually creating these meshes over the course of months. Nevertheless, some manual work is still required to make the mesh physics-ready – though this may be greatly reduced by spending more time upfront with the survey design to ensure the object of interest is properly photographed. Selecting photogrammetry software tools which are more robust to poorer acquisitions may further aid the process.

The way forward includes further workflow automation and determining how to more adaptively discretize the mesh such that we use fewer elements. Ideally, we envisage employing this methodology on structures lacking computer models, including historical structures in earthquake-prone regions. Up to this point, we have described a forward modelling process in response to a source. Naturally, using ambient or active vibrations to then invert for 3D elastic field parameters and possibly detect time-lapse changes at intermediate scales within such structures would be among the next steps to investigate.

DOI: 10.3217/978-3-99161-057-1-013

ACKNOWLEDGMENTS

The authors wish to thank ETH Zurich for its support.

REFERENCES

[1] Courant, R., K. Friedrichs, and H. Lewy. "On the partial difference equations of mathematical physics." *IBM journal of Research and Development* 11, no. 2 (1967): 215-234.
[2] Igel, H. *Computational seismology: a practical introduction*. Oxford University Press, 2017.
[3] Szeliski, R. *Computer vision: algorithms and applications*. Springer Nature, 2022.
[4] Förstner, W., and B.P. Wrobel. *Photogrammetric computer vision*. Vol. 6. Switzerland: Springer International Publishing, 2016.
[5] Hartley, R. *Multiple view geometry in computer vision*. Vol. 665. Cambridge university press, 2003.
[6] Custers, B. "Drones here, there and everywhere introduction and overview." *The future of drone use: Opportunities and threats from ethical and legal perspectives* (2016): 3-20.
[7] Kovanič, Ľ., B. Topitzer, P. Peťovský, P. Blišťan, M.B. Gergeľová, and M. Blišťanová. "Review of photogrammetric and lidar applications of UAV." *Applied Sciences* 13, no. 11 (2023): 6732.
[8] Spicher, A., and E. Wenk. "Erläuterungen zu Geologischer Atlas der Schweiz, 1: 25'000, Blatt 1313, Bellinzona." *Schweiz. Geol. Komm* (1981): Atlasblatt 66.
[9] Pfeifer, H.-R., H. Kobe, A. Colombi, D. Pozzorini, A. Steck, and Y. Gouffon. "Blatt 1312 Locarno.-Geol. Atlas Schweiz 1: 25'000, Erläuterungen 159." *Geologischer Atlas der Schweiz 1: 25'000* (2018).
[10] Lowe, D.G. "Object recognition from local scale-invariant features." In *Proceedings of the seventh IEEE international conference on computer vision*, vol. 2, pp. 1150-1157. Ieee, 1999.
[11] Afanasiev, M., C. Boehm, M.v. Driel, L. Krischer, M. Rietmann, D.A. May, M.G. Knepley, and A. Fichtner. "Modular and flexible spectral-element waveform modelling in two and three dimensions." *Geophysical Journal International* 216, no. 3 (2019): 1675-1692.
[12] Liu, Y., J. Teng, T. Xu, and J. Badal. "Higher-order triangular spectral element method with optimized cubature points for seismic wavefield modeling." *Journal of Computational Physics* 336 (2017): 458-480.
[13] Ferroni, A., P.F. Antonietti, I. Mazzieri, and A. Quarteroni. "Dispersion-dissipation analysis of 3-D continuous and discontinuous spectral element methods for the elastodynamics equation." *Geophysical Journal International* 211, no. 3 (2017): 1554-1574.
[14] Blender Development Team. (2023). Blender (Version 4.0.2) [Computer software]. https://www.blender.org
[15] Coreform Cubit (Version 2024.8) [Computer software]. Orem, UT: Coreform LLC. Retrieved from http://coreform.com
[16] Anggraeni, D. "Modelling the impact of topography on seismic amplification at regional scale." Master's thesis, University of Twente, 2010.
[17] Castellazzi, G., A.M. D'Altri, S.d. Miranda, F. Ubertini, G. Bitelli, A. Lambertini, I. Selvaggi, and A. Tralli. "A mesh generation method for historical monumental buildings: an innovative approach." In *Proceedings of the VII european congress on computational methods in applied sciences and engineering (ECCOMAS Congress 2016), Crete Island*. 2016.
[18] Baker, J., B. Bradley, and P. Stafford. *Seismic hazard and risk analysis*. Cambridge University Press, 2021.